

Measurement of Meissner effect in micro-sized Nb and FeSe crystals using an NbN nano-SQUID

This content has been downloaded from IOPscience. Please scroll down to see the full text.

2017 Supercond. Sci. Technol. 30 074011

(<http://iopscience.iop.org/0953-2048/30/7/074011>)

View [the table of contents for this issue](#), or go to the [journal homepage](#) for more

Download details:

IP Address: 202.120.224.95

This content was downloaded on 18/06/2017 at 11:28

Please note that [terms and conditions apply](#).

You may also be interested in:

[Evaluation of the intragrain critical current density in a multidomain FeSe crystal by means of dc magnetic measurements](#)

A Galluzzi, M Polichetti, K Buchkov et al.

[Anisotropic magnetic responses of a 2D-superconducting Bi₂Te₃/FeTe heterostructure](#)

Qing Lin He, Mingquan He, Junying Shen et al.

[Investigation of the vortex dynamics of Fe_{1.02}Se crystals by fundamental and 3rd harmonic ac magnetic susceptibility analysis](#)

K Buchkov, M Polichetti, K Nenkov et al.

[Magnetic field imaging of a tungsten carbide film by scanning nano-SQUID microscope](#)

Yusuke Shibata, Shintaro Nomura, Ryosuke Ishiguro et al.

[Magnetic field modulated microwave spectroscopy across phase transitions and the search for new superconductors](#)

Juan Gabriel Ramírez, Ali C Basaran, J de la Venta et al.

[Magnetic properties of fullerene superconductors](#)

V Buntar and H W Weber

[Study of the superconducting properties of the new intermetallic compound](#)

$\text{\$}\{\{\text{Zr}}\}_{1-x}\{\{\text{Nb}}\}_x\{\{\text{B}}\}_2\}\text{\$}$

M D R Marques, F S Portela, L T Corredor et al.

[NanoSQUIDs based on Niobium Nitride films](#)

R Russo, E Esposito, A Crescitelli et al.

Measurement of Meissner effect in micro-sized Nb and FeSe crystals using an NbN nano-SQUID

Long Wu^{1,2}, Lei Chen^{1,5}, Hao Wang^{1,2}, Qisi Wang³, Hongliang Wo³, Jun Zhao³, Xiaoyu Liu¹, Xiaolei Wu^{1,2} and Zhen Wang^{1,2,4,5}

¹ CAS Center for Excellence in Superconducting Electronics(CENSE), State Key Laboratory of Functional Material for Informatics, Shanghai Institute of Microsystem and Information Technology (SIMIT), Chinese Academy of Sciences (CAS), Shanghai 200050, People's Republic of China

² University of Chinese Academy of Science, Beijing 100049, People's Republic of China

³ The Department of Physics, Fudan University, Shanghai, 200433, People's Republic of China

⁴ School of Physical Science and Technology, ShanghaiTech University, Shanghai 200031, People's Republic of China

E-mail: leichen@mail.sim.ac.cn and zwang@mail.sim.ac.cn

Received 26 February 2017, revised 11 April 2017

Accepted for publication 4 May 2017

Published 14 June 2017



CrossMark

Abstract

The nano-superconducting quantum interference device (SQUID) is considered one of the most sensitive magnetic sensors for the characterization of mesoscopic and microscopic magnetic moments. Therefore, it is suitable for measuring the Meissner effect in small superconductors that cannot generate large enough signals for commercial magnetometers. To achieve an optimized coupling, the sample is usually placed directly on a SQUID chip and as close to the SQUID washer as possible. Therefore, a large working temperature range of the nano-SQUID is desirable to measure a wider range of samples. Here, we achieved the measurement of the Meissner effect in a 25 μm -sized Nb and a 40 $\mu\text{m} \times 120 \mu\text{m}$ -sized FeSe crystals using a niobium nitride (NbN) nano-SQUID. This nano-SQUID has a usable magnetic flux modulation for temperatures up to 9.5 K. The flux noise is around 50–60 $\mu\Phi_0 \text{ Hz}^{-1/2}$ for the entire measurement system. The diamagnetic branches induced by the Meissner effect below the lower critical field were observed for both Nb and FeSe crystals with the NbN nano-SQUID device. In addition, at various temperatures, strong magnetic hysteresis arising from vortices pinning was also observed and analyzed for both Nb and FeSe crystals.

Keywords: NbN nano-SQUID, Meissner effect, magnetic hysteresis, micro-sized FeSe crystal

(Some figures may appear in colour only in the online journal)

1. Introduction

With superconductivity moving towards smaller scales and lower dimensions, many emergent phenomena [1–3] appear such as the Little–Parks effect [4], oscillations in critical temperature T_c with film thickness [5], and half-integer flux quanta steps in a superconducting ring [6]. However, many of these interesting effects require a sensitive near-field magnetic characterization. For example, ferromagnetism and

superconductivity at the interface of LaAlO_3 and SrTiO_3 was discovered to coexist using a scanning superconducting quantum interference device (SQUID) technique [7]. Recently, a three-axis nano-SQUID was even developed for direct on-chip measurement of a vector magnetic moment [8]. With a nano-SQUID, the sensitivity of magnetic moment improves by around ten orders of magnitude compared with a commercial magnetometer system [9–13]. The reason is that the nano-SQUID has a miniaturized SQUID washer that couples to the samples directly [13–16]. The critical temperature T_c of the nano-SQUID limits the working-temperature

⁵ Authors to whom any correspondence should be addressed.

range of an on-chip nano-SQUID measurement. Here, we used a NbN nano-SQUID that has a working temperature range of up to 9.5 K, which covers the superconducting transition temperature of many interesting materials like Nb and FeSe. Nb is a type-II superconductor widely used in superconducting electronics, and its magnetic behavior is highly correlated to the flux noise of the device [17]. Structurally, FeSe is the simplest iron-based superconductor, and its superconducting properties are also presumably related to its magnetism [18].

We have achieved measurements of the Meissner effect in both Nb and FeSe micro-sized crystals using our customized NbN nano-SQUID installation. The nano-SQUID measurement results for a single Nb crystal features a large magnetic hysteresis in the superconducting state, in contrast with those from a commercial magnetometer (MPMS, Quantum Design) for a large ensemble of Nb crystals. Furthermore, with NbN nanoSQUID measurements, a large magnetic hysteresis is observed for both the bulk and micro-sized FeSe crystals in their superconducting state. However, the hysteresis of the micro-sized crystal is more sensitive to temperature than the bulk crystal. In contrast, the lower critical field H_{c1} of the bulk FeSe crystal is less than that for the micro-sized crystal.

2. Methods

The NbN nano-SQUID used here (inset in figure 1(a)) was fabricated using a method similar to a 3D Nb nano-SQUID [19, 20]. A 16 nm wide insulating slit was formed within the NbN washer using a unique lift-off process. Next, two parallel nano-bridge junctions of 100 nm width were set across the insulating slit forming a SQUID with a loop size of $1 \mu\text{m} \times 1 \mu\text{m}$. In this type of 3D nano-SQUID, the nano-bridge junctions (of 15 nm thickness) are much thinner than the SQUID loop (of 150 nm thickness), and hence that the magnetic flux modulation is deeper relative to the planar device. Although the short coherence length of NbN (~ 5 to 7 nm) places a great challenge on device fabrication, the critical temperature T_c of a NbN device is higher than that of a Nb device. The NbN nanoSQUID exhibits a usable magnetic flux interference pattern for temperatures up to 9.5 K. The critical current at for constructive $I_{c\text{-max}}$ and destructive $I_{c\text{-min}}$ interference as a function of temperature T is plotted in figure 1(a). As the fabrication of the NbN nano-SQUID is still crude and the device has a large critical current, there is a hysteresis in the current–voltage curves because of thermal heating. In this case, we used a pulsed-current bias method to avoid the hysteresis in the measurement [21, 22]. Briefly, a constant number N_{pulse} of current pulses of amplitude I_{pulse} is sent to the nano-SQUID. Then, the corresponding voltage pulses $V_{\text{sw},j}$ across the SQUID are recorded. The switched voltage pulse number N_{sw} was counted provided $V_{\text{sw},j}$ is greater than a threshold voltage; the switching probability was evaluated using $P_{\text{sw}} = N_{\text{sw}}/N_{\text{pulse}}$. Figure 1(b) gives P_{sw} as a function of I_{pulse} as well as I_{coil} , which is the current applied to the feedback coil placed

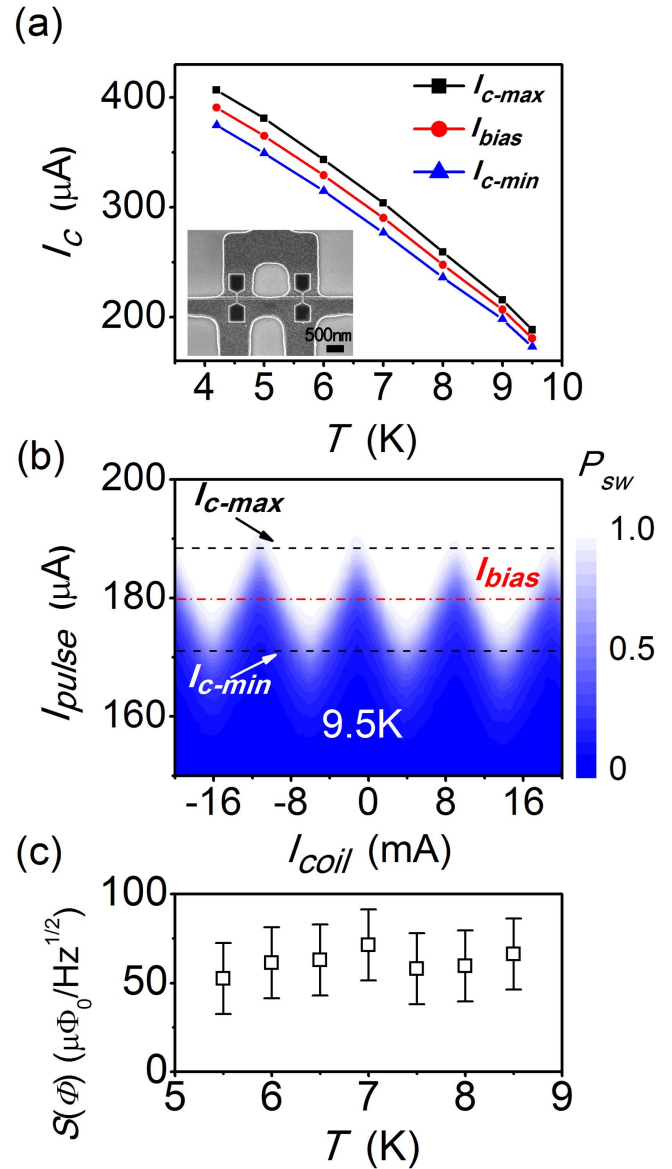


Figure 1. (a) Critical current I_c of the NbN nano-SQUID as a function of temperature T for constructive $I_{c\text{-max}}$ (black square) and destructive $I_{c\text{-min}}$ (blue triangle) interference. The inset shows a scanning electron microscope image of the NbN nano-SQUID. (b) Contour map of P_{sw} as the function of I_{pulse} and I_{coil} at $T = 9.5$ K. (c) Magnetic flux noise density $S(\Phi)$ of the entire nanoSQUID installation at various temperatures.

above the nano-SQUID. A clear interference pattern in P_{sw} is observed at 9.5 K. By biasing the nano-SQUID with a current pulse of amplitude I_{bias} that is in between $I_{c\text{-max}}$ and $I_{c\text{-min}}$, we are able to measure the flux noise at various temperatures. As seen in figure 1(c), the flux noise is around $50\text{--}60 \mu\Phi_0 \text{Hz}^{-1/2}$ and shows no dependence on temperature. Actually, the flux noise is still limited by noise from our room-temperature readout installation and has not yet reach the SQUID thermal noise. With further improvements in device fabrication and suppression of instrumental noise, another two orders of magnitude enhancement is expected. Several state-of-the-art nanoSQUIDs have been reported

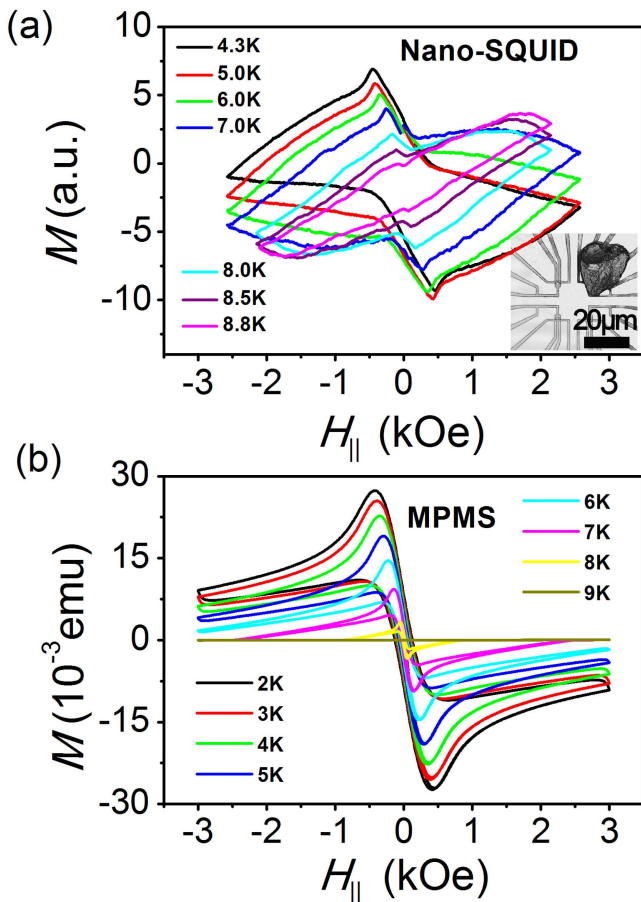


Figure 2. (a) M - H_{\parallel} curves at various temperatures measured using the NbN nano-SQUID. The inset shows an image of one Nb crystal on the chip of a NbN nanoSQUID. (b) M - H_{\parallel} curves at various temperatures measured with the MPMS magnetometer.

with intrinsic flux noise below $50 n\Phi_0 \text{ Hz}^{-1/2}$ [11, 23, 24]. However, even at the current noise performance, the NbN nano-SQUID installation already is able to measure the magnetization of micro-sized superconductors of higher critical temperatures, such as the Nb and FeSe crystals.

3. Results and discussion

To measure the Meissner effect of a micro-sized Nb crystal, the sample is placed close to the NbN nano-SQUID on the chip and cooled to a low temperature in a variable temperature insert probe. The size of the Nb crystal is around $25 \mu\text{m}$ (see inset of figure 2(a)). The magnetization M as a function of magnetic field H_{\parallel} parallel to the SQUID plane is plotted in figure 2(a). At $T = 4.3 \text{ K}$, as H_{\parallel} is swept from 0 toward 2.5 kOe , the M - H_{\parallel} curve (black line) moves from a negative dM/dH_{\parallel} (diamagnetic) regime to a positive dM/dH_{\parallel} (paramagnetic) regime at the lower critical field $H_{c1} = 0.46 \text{ kOe}$. The H_{c1} decreases as the temperature increases, and so does the magnetic hysteresis. The behavior is in accordance with the properties of type-II superconductors. In the diamagnetic

regime, the magnetic field is expelled from the Nb particle (the Meissner effect), whereas in the paramagnetic regime, vortices are trapped and accumulate inside the crystal.

For a comparison with our NbN nano-SQUID measurements, we used the MPMS magnetometer to measure the magnetization curves of a Nb particle ensemble (of about 1900 particles) at various temperatures (figure 2(b)). Similar transitions from the diamagnetic regime to paramagnetic regime in M - H_{\parallel} curves of a typical type-II superconductor are observed, although there are differences in the details. First, the turning point H_{c1} is sharper in the single-particle measurement; the variation in the individual crystals in a large ensemble broadens the transition from the diamagnetic to the paramagnetic regime. Second, the magnetic hysteresis shows a more open loop for a single crystal measured using the NbN nano-SQUID compared with the results of MPMS measurements for the large ensemble. For materials with a Ginzburg-Landau parameter $\kappa > 1/\sqrt{2}$, the pinning of vortices inside the superconductor above H_{c1} neutralizes the diamagnetism and induces magnetic hysteresis. For a large ensemble, the outer crystals in the cluster may act as a magnetic shield to the inner crystals and lessen the total pinning effect of vortices. Therefore, the measurements from one Nb crystal using the NbN nano-SQUID not only delivers a more accurate H_{c1} characterization, but also offers more raw information about vortices pinning.

Besides micro-sized Nb crystals, we also used the NbN nano-SQUID to measure both bulk and micro-sized FeSe crystals. The bulk FeSe single crystal (figure 3(c)) was grown under a permanent gradient temperature ($\sim 400 \text{ }^{\circ}\text{C}$ to $330 \text{ }^{\circ}\text{C}$) in a KCl-AlCl₃ flux. The micro-sized FeSe crystal (figure 3(d)) is a flake cleaved from the bulk crystal using the tip of a pair of ceramic tweezers, and attached to the nano-SQUID chip with a small quantity of N grease.

The nano-SQUID and sample were cooled to a low temperature at zero field. The parallel magnetic field M - H_{\parallel} was swept from 0 to $\sim 200 \text{ Oe}$ (figure 3(a)), then reversed to $\sim -200 \text{ Oe}$, and back to $\sim 200 \text{ Oe}$ to complete a loop. Unlike the Nb crystal, vortices pinning in the FeSe sample is permanent after applying a magnetic field. Therefore, before each M - H_{\parallel} curve measurement, the SQUID and sample were heated up to 18 K , well above T_c for FeSe, to remove trapped vortices and then re-cooled to the targeted temperature at zero field.

The original M - H_{\parallel} curves at various temperatures for the micro-sized FeSe sample measured by NbN nano-SQUID are plotted in figure 4. In order to evaluate the magnetic hysteresis alone, we performed the following mathematical analysis. The symmetric hysteresis curves in figure 3(b) were acquired by subtracting the background curves in figure 3(g) from the original M - H_{\parallel} curves respectively. The background curves in figure 3(g) were calculated from averages of M at the same H_{\parallel} on the upper and lower sections of the hysteresis curve in figure 4. We believe that the symmetric magnetic hysteresis curves are originated from the Meissner effect of the micro-sized FeSe crystal.

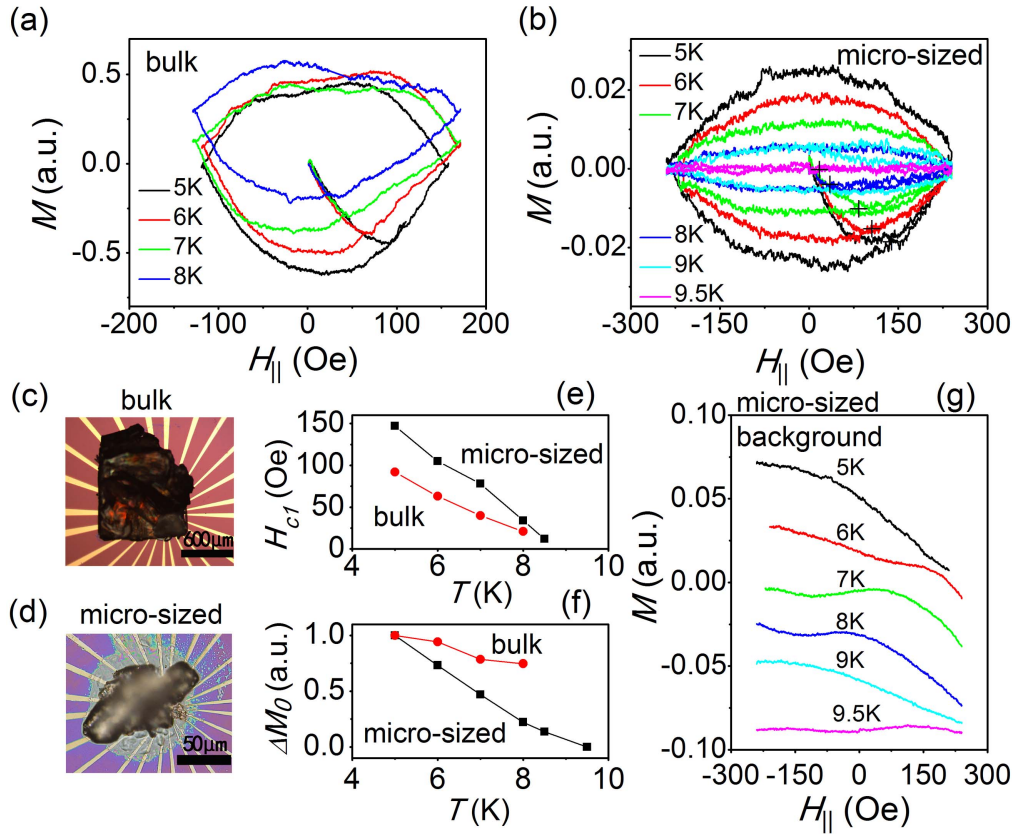


Figure 3. NbN nano-SQUID measured $M-H_{||}$ curves of (a) a bulk FeSe crystal and (b) a micro-sized crystal, at various temperatures after the subtraction of background in figure 3(g). (c) Image of the bulk FeSe crystal. (d) Image of the micro-sized FeSe crystal. (e) Lower critical field H_{c1} as a function of temperature for the bulk (red dot) and micro-sized (black square) crystals. (f) Normalized magnetic hysteresis size at zero field ΔM_0 as a function of temperature for the bulk (red dot) and micro-sized (black square) crystals. (g) Background of the $M-H_{||}$ curves for the micro-sized crystal at various temperatures.

For both the bulk and micro-sized FeSe crystal, a diamagnetic regime of negative $dM/dH_{||}$ from zero field was observed (figures 1(a) and (b)). Then, the $M-H_{||}$ curves form closed hysteresis loops in sweeping $H_{||}$ back and forth. Here, lower critical field H_{c1} is acquired by the $H_{||}$ value at the intersection point (black cross) of the initial diamagnetic branch and the hysteresis loop. The temperature dependence of H_{c1} (figure 3(e)) for both bulk and micro-sized crystal indicate that the H_{c1} for the latter is greater, and diverge to zero at $T_c = 8.7$ K. Since the micro-sized crystal is much thinner than the bulk one, vortices are more difficult to penetrated the thinner sample under the parallel magnetic field.

In figure 3(f), the normalized size of magnetic hysteresis ΔM_0 of the bulk and micro-sized crystal was the hysteresis size ΔM at various temperature normalized to their ΔM at $T = 5$ K respectively. Here, the ΔM is the difference in M on the upper and lower section of the magnetic hysteresis loop at zero field in figure 3(b). As T increases, the normalized hysteresis size ΔM_0 for the micro-sized crystal drops quickly, but that for the bulk stays relatively constant. The pinning force of vortices in small crystals is therefore more sensitive to temperature in comparison with that in the bulk one. It might indicate the vortices pinning is more stable for the large crystal than the micro-sized one. In figure 3(g), the

background curves shows no particular dependence on temperature. We suspect that the irregular background magnetization probably stems from the magnetic impurities in the N grease or in the samples.

4. Conclusion

In summary, the fabricated NbN nano-SQUID exhibited a usable flux modulation for temperatures up to 9.5 K. The expanded working temperature of the NbN nano-SQUID enabled more accurate measurements to be made of the Meissner effect in micro-sized Nb and FeSe crystals. In both samples, a diamagnetic regime was observed by sweeping the field from zero to H_{c1} . Also, comparing the NbN nano-SQUID-measured results of micro-sized Nb crystals with MPMS-measured results of a large ensemble of Nb crystals, we found that the NbN nano-SQUID measurements not only delivered a more accurate H_{c1} characterization, but also offered more raw information on vortices pinning. We also performed a comparison of the micro-sized FeSe single crystal with a bulk crystal using the NbN nano-SQUID measurements. The result indicated that the pinning force of the vortices in the micro-sized crystal has a stronger dependence on temperature than that for the bulk crystal.

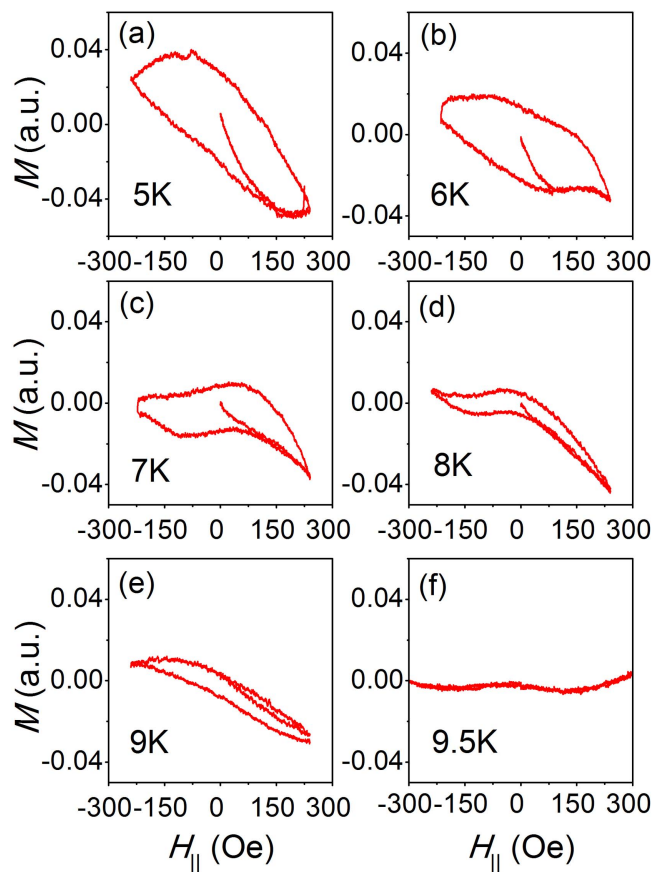


Figure 4. (a)–(f) Original data of the NbN nano-SQUID-measured magnetization of the micro-sized FeSe crystal as a function of magnetic field at various temperatures.

Moreover, the lower critical field H_{c1} of the bulk FeSe crystal is less than the micro-sized crystal. In the future, further optimizations are to be made in the fabrication of the NbN nano-SQUID and noise performance in the readout installation. The flux noise of the whole measurement system can be further improved. In that case, the magnetic measurement of a single-unit-cell thick FeSe film using a NbN nano-SQUID would be extremely interesting.

Acknowledgments

We gratefully acknowledge support from the Strategic Priority Research Program of the Chinese Academy of

Sciences (Grant No. XDB04000000), as well as funding from the National Science Foundation of China (Grant No. 61306151).

References

- [1] Geim A K, Dubonos S V, Lok J G S, Henini M and Maan J C 1998 *Nature* **396** 144–6
- [2] Bose S, Garcia-Garcia A M, Ugeda M M, Urbina J D, Michaelis C H, Brihuega I and Kern K 2010 *Nat. Mater.* **9** 550–4
- [3] Jiang D *et al* 2014 *Nat. Commun.* **5** 5708
- [4] Staley N E and Liu Y 2012 *Proc. Natl Acad. Sci.* **109** 14819–23
- [5] Guo Y *et al* 2004 *Science* **306** 1915–7
- [6] Jang J, Ferguson D G, Vakaryuk V, Budakian R, Chung S B, Goldbart P M and Maeno Y 2011 *Science* **331** 186
- [7] Bert J A, Kalisky B, Bell C, Kim M, Hikita Y, Hwang H Y and Moler K A 2011 *Nat. Phys.* **7** 767–71
- [8] Martínez-Pérez M J, Gella D, Müller B, Morosh V, Wölbing R, Sesé J, Kieler O, Kleiner R and Koelle D 2016 *ACS Nano* **10** 8308–15
- [9] Granata C and Vettoliere A 2016 *Phys. Rep.* **614** 1–69
- [10] Ketchen M B, Awschalom D D, Gallagher W J, Kleinsasser A W, Sandstrom R L, Rozen J R and Bumble B 1989 *IEEE Trans. Magn.* **25** 1212–5
- [11] Vasyukov D *et al* 2013 *Nat. Nano* **8** 639–44
- [12] Schwarz T, Wölbing R, Reiche C F, Müller B, Martínez-Pérez M J, Mühl T, Büchner B, Kleiner R and Koelle D 2015 *Phys. Rev. Appl.* **3** 044011
- [13] Tilbrook D L 2009 *Supercond. Sci. Technol.* **22** 064003
- [14] Wernsdorfer W 2009 *Supercond. Sci. Technol.* **22** 064013
- [15] Granata C, Esposito E, Vettoliere A, Petti L and Russo M 2008 *Nanotechnology* **19** 275501
- [16] Wölbing R, Schwarz T, Müller B, Nagel J, Kemmler M, Kleiner R and Koelle D 2014 *Supercond. Sci. Technol.* **27** 125007
- [17] Clarke J and Braginski A I 2004 *The SQUID Handbook* vol 1 (Weinheim: Wiley-VCH) ch 3
- [18] Wang Q *et al* 2016 *Nat. Commun.* **7** 12182
- [19] Chen L, Wang H, Liu X, Wu L and Wang Z 2016 *Nano Lett.* **16** 7726–30
- [20] Wang H, Chen L, Liu X, Wu L, Wu X, You L and Wang Z 2017 *IEEE Trans. Appl. Supercond.* **27** 1–5
- [21] Wu L, Chen L, Wang H, Liu X and Wang Z 2017 *Sci. Rep.* **7** 45945
- [22] Chen L, Wernsdorfer W, Lampropoulos C, Christou G and Chiorescu I 2010 *Nanotechnology* **21** 405504
- [23] Schwarz T, Nagel J, Wölbing R, Kemmler M, Kleiner R and Koelle D 2013 *ACS Nano* **7** 844–50
- [24] Levenson-Falk E M, Vijay R, Antler N and Siddiqi I 2013 *Supercond. Sci. Technol.* **26** 055015